Characterization of the Microchemical Structure of Seed Endosperm within a Cellular Dimension among Six Barley Varieties with Distinct Degradation Kinetics, Using Ultraspatially Resolved Synchrotron-Based Infrared Microspectroscopy

Na Liu and Peiqiang Yu*

College of Agriculture and Bioresources, University of Saskatchewan, Saskatoon, SK, Canada S7N 5A8

Barley varieties have similar chemical composition but exhibit different rumen degradation kinetics and nutrient availability. These biological differences may be related to molecular, structural, and chemical makeup among the seed endosperm tissue. No detailed study was carried out. The objectives of this study were: (1) to use a molecular spectroscopy technique, synchrotron-based Fourier transform infrared microspectroscopy (SFTIRM), to determine the microchemical−structural features in seed endosperm tissue of six developed barley varieties; (2) to study the relationship among molecular−structural characteristics, degradation kinetics, and nutrient availability in six genotypes of barley. The results showed that inherent microchemical−structural differences in the endosperm among the six barley varieties were detected by the synchrotron-based analytical technique, SFTIRM, with the univariate molecular spectral analysis. The SFTIRM spectral profiles differed ($P < 0.05$) among the barley samples in terms of the peak ratio and peak area and height intensities of amides I (ca. 1650 cm^{-1}) and II (ca. 1550 cm^{-1}), cellulosic compounds (ca. 1240 cm^{-1}), CHO component peaks (the first peak at the region ca. 1184−1132 cm^{-1}, the second peak at ca. 1132−1066 cm^{-1}, and the third peak at ca. 1066−950 cm^{-1}). With the SFTIRM technique, the structural characteristics of the cereal seeds were illuminated among different cultivars at an ultraspatial resolution. The structural differences of barley seeds may be one reason for the various digestive behaviors and nutritive values in ruminants. The results show weak correlations between the functional groups' spectral data (peak area, height intensities, and ratios) and rumen biodegradation kinetics (rate and extent of nutrient degradation). Weak correlations may indicate that limited variations of these six barley varieties might not be sufficient to interpret the relationship between spectroscopic information and the nutrient value of barley grain, although significant differences in biodegradation kinetics were observed. In conclusion, the studies demonstrated the potential of ultraspatially resolved synchrotron based technology (SFTIRM) to reveal the structural and chemical makeup within cellular and subcellular dimensions without destruction of the inherent structure of cereal grain tissue.

KEYWORDS: Synchrotron; degradation kinetics; microchemical structure; endosperm

INTRODUCTION

Barley varieties exhibit different ruminal degradation rates and kinetics features (*1, 2*). Knowledge of their chemical and structural differences may lead to an understanding of the reasons for these differences in degradation kinetics. Further study of the relationship of biological characteristics (in terms of biodegradation kinetics) of barley grain in relation to spectral−structural characteristics may provide useful understanding of how to best utilize the various barley varieties.

In conventional chemical analysis, harsh chemical reagents can unavoidably destroy or even obliterate the histological structure of the biological sample (*3−5*). The detection of inherent structural and chemical information is beyond the capacity of traditional chemical analysis, owing to the destructive pretreatment and the treatment during chemical analysis. These disadvantages necessitate a new and rapid tool to overcome the limitations.

Conventional (globar-sourced) FTIR microspectroscopy shows comparable performance to synchrotron only when working with large aperture size (> 30−50 μm) (*5, 6*). However, it is inferior to synchrotron at an ultraspatial resolution when detecting biological or biomedical specimens (5−20 μm) (*7−10*). To overcome the weakness of conventional (thermal) light source, brilliant synchrotron light (which is million times brighter than

*Corresponding author. College of Agriculture and Bioresources, University of Saskatchewan, 6D10 Agriculture Building, 51 Campus Drive, Saskatoon, SK, Canada S7N 5A8. Tel: +1 306 966 4132. E-mail: peiqiang.yu@usask.ca.

sun light) is used because it is extremely advantageous for small aperture settings (*11*).

Synchrotron radiation allows simultaneous sample viewing and IR data collection at ultraspatial resolution. Using the synchrotron source to substitute for a conventional thermal (globar) source results in the potential to improve the S/N ratio and reach the diffraction limit (*8, 11–13*). The combining of microscopy with FTIR spectroscopy enables observations both visually and spectroscopically. Ultraspatially resolved synchrotron FTIR microspectroscopy is used to monitor the intrinsic distribution of chemical compounds in biological and biomedical specimens (*14*). Accordingly, taking advantage of the brilliance, broadband, and concentration (*11*), the application of synchrotron light associated with the FTIR technique makes it possible to probe further on the inherent structure of biological materials at a cellular or subcellular dimension without thermal noise (*15*).

The synchrotron-based FTIRM technique may enable us to establish a correlation of spectral information to structural and chemical features of plant/seed tissues, furthermore, to feed/food quality. The objectives of this study were (1) to use synchrotron-based FTIR microspectroscopy to determine structural makeup features and identify the structural differences in chemical functional groups in endosperm tissue within a cellular dimension among the six developed barley varieties; (2) to analyze the correlation between biodegradation kinetics (rate and extent of rumen degradation) and chemical functional group features determined by the synchrotron-based FTIR microspectroscopy.

MATERIALS AND METHODS

Barley Varieties and Growth Conditions. Six barley varieties were used in this study, including AC Metcalfe (for malting purposes), CDC Dolly (for feed purposes), McLeod (for feed purposes), CDC Helgason (for feed purposes), CDC Trey (for feed purposes), and CDC Cowboy (for feed and forage dual purposes). All are two-row hulled spring barley varieties. AC Metcalfe has a higher yield and larger and more plump seeds than Harrington. CDC Dolly is widely grown in Canada for its high test weight and plumpness. McLeod is developed with good yield and higher test and kernel weight than Harrington. CDC Helgason has similar plumpness but a higher yield and test weight compared to those of CDC Dolly. CDC Trey is suitable for growing in the eastern Canada prairies with large, plump seeds. CDC Cowboy has high biomass but somewhat lower grain yield (Rossnagel, B. G., personal communication (*16, 17*)).

The year of the barley grain harvest was 2005. The climate conditions during the year were 17.5 °C mean maximum daily temperature and 455 mm rainfall. Barley samples were obtained from Crop Development Center (CDC), University of Saskatchewan. All barley varieties were grown without irrigation at Kernen Crop Research Farm, University of Saskatchewan, Canada, following standard agronomic production practices for barley production.

In situ rumen degradation kinetics (degradation rate and extent) were significantly different among these barley varieties, as presented in **Table 1**. These data were used for the correction study between the degradation rate and extent and spectral structural features at the endosperm region in the barley varieties, revealed by the ultraspatially resolved synchrotron-based FTIR microspectroscopy within a cellular dimension.

Sample Preparation for Synchrotron-Based FTIR Microspectroscopy. Five seeds of each barley variety (six varieties) were randomly selected to cut transversely across the endosperm tissue using a microtome at Western College of Veterinary, University of Saskatchewan, Saskatoon, Canada. The thin cross-sections of tissues (6 μm) were unstained and mounted on barium fluoride (BaF_2) discs (2 mm thick, 13 mm diameter; Spectral Systems, Hopewell Junction, NY, USA) for synchrotron FTIR microspectroscopic work in transmission mode. The detailed methodology was reported by Yu et al. (*14, 18*).

Synchrotron Radiation Sources and Synchrotron FTIR Microspectroscopy. The synchrotron FTIRM experiment was performed using a Thermo Nicolet Magna 860 Step-Scan FTIR (Thermo Fisher Scientific Inc., Waltham, MA) spectrometer equipped with a Spectra Tech

Continuum IR Microscope (Spectra-Tech, Inc., Shelton, CT) and liquid nitrogen-cooled mercury cadmium telluride (MCT) detector. The IR microspectroscopy instrument was coupled with synchrotron radiation from U2B beamline, National Synchrotron Light Source, Brookhaven National Laboratory, U.S. Department of Energy (NSLS-BNL, Upton, NY).

Synchrotron FTIRM Data Collection and Processing. The spectra were collected from five seeds of each barley variety. Spot samples (30–60) were randomly selected in the endosperm region between 100 and 600 μm from outside of the seed section on each window according to the method reported by Walker et al. (*19*). The spectra were collected through an aperture of 10×10 μm in transmission mode within mid-IR spectral range of ca. 4000–800 cm^{-1}. The spatial resolution was set as 4 cm^{-1}, and 128 scans were co-added to each spot to produce an IR spectrum. Background spectra were collected using the same measurement setting. Atlus software (Thermo Nicolet, Madison, WI, USA) was used to produce the visual image of the sample. Nicolet OMNIC software 7.3 (Spectra Tech, Madison, WI, USA) was used to collect and analyze spectral data. After baseline correction, the absorption peak parameters (baseline, region, relative height, and area) were recorded for further univariate analysis (*13*). More details on SFTIRM data collection were documented in Marinkovic et al. (*8*) and Yu et al. (*20*).

Statistical Analysis. Statistical analyses were performed using the MIXED procedure of SAS 9.1.3 (SAS Institute, Inc., Cary, NC). Fisher's protected test was used to compare means with $P < 0.05$, which were considered significant.

The synchrotron FTIRM data were analyzed using a completed nested design. The model used for the analysis was: $Y_{ij} = \mu + T_i + S(T)_j + e_{ij}$, where Y_{ij} was an observation of the dependent variable *ij*; μ was the population mean for the variable; T_i was the effect of the barley varieties, as a fixed effect; $S(T)_j$ was the seeds nested within treatments, as a random effect; and e_{ij} was the random error associated with the observation *ij*. The detailed methodology was reported in Yu (*9*) and Doiron et al. (*21, 22*).

The correlation between the degradation rate and extent of dry matter (DM), crude protein (CP), starch (ST), and synchrotron FTIRM spectral characteristics among the six barley varieties was analyzed using the CORR procedure of SAS software.

RESULTS AND DISCUSSION

Using Synchrotron-Based FTIR Microspectroscopy to Characterize and Compare Microchemical−Structural Makeup of Seed Endosperm Tissue within a Cellular Dimension among Six Barley Varieties. The synchrotron FTIRM technique was used to characterize inherent seed microchemical structure (*23*) among these six barley varieties. The spectra observed in the region of ca. 4000–800 cm^{-1} were analyzed to show the absorption characteristics attributed to the chemical functional groups of barley grains.

For synchrotron FTIRM, the barley seed specimens were optically observed with the coupled microscope, and spot sampling was done randomly on endosperm tissue (between 100 and 600 μm from outside of the seed section) of each barley variety to produce the spectral data. **Figure 1a** illustrates the typical SFTIRM spectrum of the endosperm tissue in the region of ca. 4000–800 cm^{-1}. The IR spectra of characteristic bands associated with specific nutrients (protein, cellulosic compounds in **Figure 1**, and carbohydrates in **Figure 2**) are shown as well.

The characteristic absorbance bands of the amide groups can be used to probe and characterize the structural and chemical makeup of the plant tissue. The amide I (ca. 1650 cm^{-1}) and amide II (ca. 1550 cm^{-1}) peak area and height definition used for the spectral univariate analysis are shown in **Figure 1c,d,e,f**. The peak centered at approximately 1240 cm^{-1} (**Figure 1g,h**) was considered to represent the structural carbohydrates (cellulosic compounds) (*12, 24, 25*). The total carbohydrate peak area is located at the region from ca. 1184 to 951 cm^{-1} because of C−O and C−C stretching vibrations and C−O−H deformation (*12, 24, 25*). The CHO band intensities were determined by

Table 1. Comparison of Six Barley Varieties: Chemical Profile and in Situ Rumen Degradation Kinetics of Dry Matter (DM), Crude Protein, and Starch (ST)

items	barley variety[a]						SEM[b]	*P* value
	AC Metcalfe	CDC Dolly	McLeod	CDC Helgason	CDC Trey	CDC Cowboy		
in situ rumen degradation kinetics of DM[c]								
K_d (%/h)	10.04 a	7.84 b	9.63 ab	5.62 c	9.72 a	8.29 ab	0.671	0.0025
EDDM (%)	48.66 a	39.49 c	45.00 b	35.98 d	49.80 a	45.46 b	0.999	<0.0001
in situ rumen degradation kinetics of CP[c]								
K_d (%/h)	6.72 a	6.18 ab	6.99 a	4.55 b	6.95 a	5.73 ab	0.551	0.0560
EDCP (%CP)	44.69 a	39.04 bc	42.56 ab	36.41 c	45.30 a	42.17 ab	1.250	0.0022
in situ rumen degradation kinetics of starch (ST)[c]								
K_d (%/h)	7.05 a	4.24 d	5.28 c	3.67 e	7.11 a	6.16 b	0.176	<0.0001
EDST (%ST)	55.04 a	41.67 d	46.79 c	38.99 e	54.27 a	50.69 b	0.870	<0.0001

[a] All six varieties of barley were grown at the Kernen Crop Research Farm (University of Saskatchewan, Saskatoon, Canada) and were managed using the same and standard agronomic production practices for all barley production (Crop Development Center). [b] SEM = standard error of mean. Means with different letters in the same row are significantly different (*P* < 0.05). [c] K_d = degradation rate; EDDM, EDCP, and EDST = effective degradability of dry matter, crude protein, and starch, respectively.
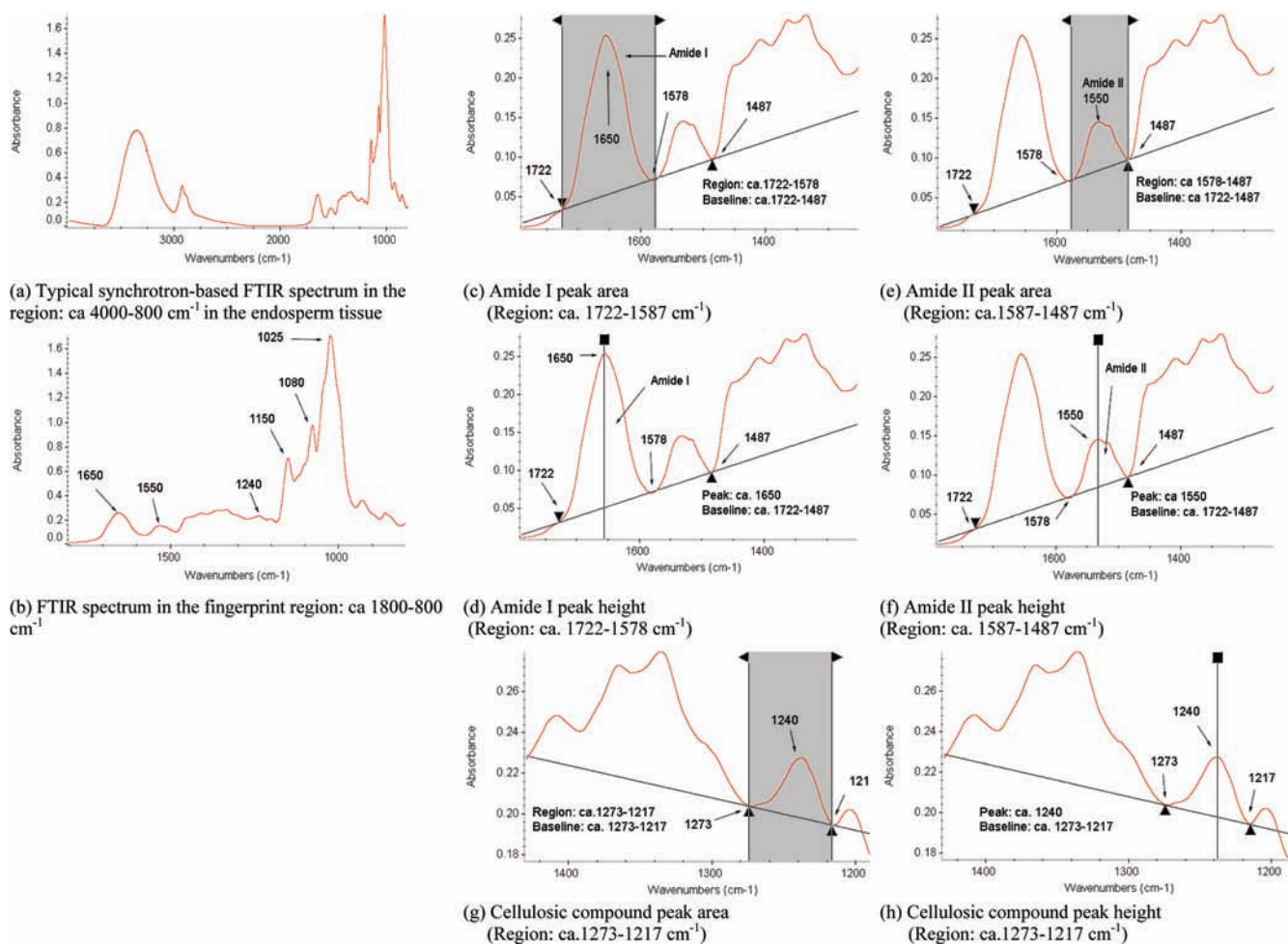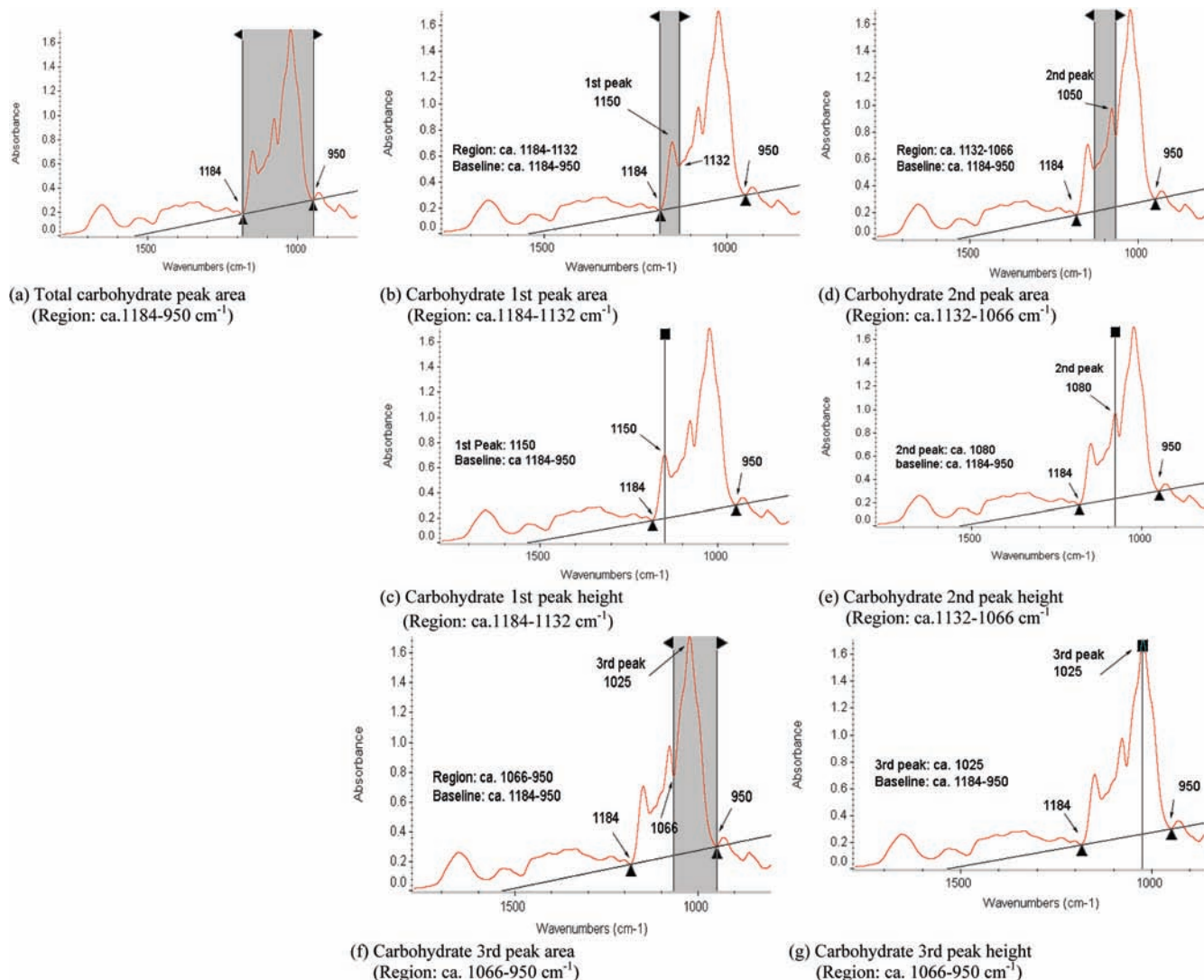

Figure 1. Typical synchrotron-based FTIR spectrum of endosperm tissue within a cellular dimension. (**a**) Whole mid-IR region: ca. 4000−800 cm^{-1}. (**b**) Fingerprint region: ca. 1800−800 cm^{-1}. (**c,d**) Amide I peak area and height: ca. 1650 cm^{-1}. (**e,f**) Amide II peak area and height: ca. 1550 cm^{-1}. (**g,h**) Cellulosic compounds peak area and height: ca. 1240 cm^{-1}.

calculating the peak heights and areas of specific bands: the carbohydrate first component peak area occurs at the region of ca. 1184−1132 cm^{-1}, the carbohydrate second component peak area occurs at the region of ca. 1132−1066 cm^{-1}, and the carbohydrate third peak area occurs at the region of ca. 1066−950 cm^{-1}. These three peaks are regarded to represent total carbohydrate compounds (**Figure 2**).

To detect the structural features associated with nutrients, synchrotron-based FTIR microspectroscopy was used to examine structure features of barley endosperm tissue. **Tables 2** and **3** show spectroscopic data from the spot samples within cellular dimensions. It needs to be mentioned that the peak intensities (e.g., amide I area and height) should not be considered as a representation of accurate biological compound content (e.g., starch and protein).

7804 *J. Agric. Food Chem.,* Vol. 58, No. 13, 2010

Liu and Yu

Figure 2. Typical synchrotron-based FTIR spectrum of endosperm tissue within a cellular dimension. (**a**) Total carbohydrate peak area region: ca. 1184−950 cm^{-1}. (**b,c**) Carbohydrate first component peak area and height: ca. 1150 cm^{-1}. (**d,e**) Carbohydrate second component peak area and height: ca. 1080 cm^{-1}. (**f,g**) Carbohydrate third component peak area and height: ca. 1025 cm^{-1}.

Structural Characteristics of Protein Amides I and II in Barley Endosperm. **Table 2** shows that McLeod had the largest ($P < 0.05$) amide I peak area (10.02 IR absorbed intensity unit), indicating a greater concentration of protein in the endosperm tissue. In contrast, CDC Helgason showed the lowest value (7.33). The other four barley varieties were in between. Six barley varieties differed ($P < 0.05$) in amide I peak height and varied from 0.11 to 0.16. McLeod exhibited the highest amide II peak area and height (2.57 and 0.05, respectively), implying a greater concentration of protein in the endosperm tissue. By analyzing the peak of the total amides I and II areas (**Table 2**), McLeod was still the greatest (12.59), while CDC Helgason was the smallest (9.19). This may partially explain the lowest effective degradability of CP of CDC Helgason among the six barley varieties (**Table 1**). If the six barley varieties are ranked on the basis of their amide group intensities, all of the amide group parameters (amide I, amide II, and total amide I and II) show a similar trend that CDC Helgason exhibited the smallest value, whereas McLeod showed the greatest peak intensity. As for the remaining four, AC Metcalfe and CDC Dolly had relatively smaller values, and CDC Trey and CDC Cowboy were relatively higher. These results agree with the previous work that McLeod was developed as a high protein content barley (*26, 27*). The protein can play a

protector role when it combined with structural and nonstructural carbohydrates (e.g., starch granule) to form a protein matrix, which is related with barley rumen degradability and total tract digestibility.

Structural Characteristics of Carbohydrates and Structural Carbohydrate in Barley Endosperm. **Table 2** shows the absorbance peak area and height intensities of the nonstructural and structural carbohydrates (cellulosic compounds) in the endosperm tissue of the six barley varieties. There were different peak intensities found in the region ca. 1184−951 cm^{-1}, revealing the various CHO contents of the endosperm tissue of barley varieties. CDC Trey had the relatively smallest peak area (0.47) at ca. 1240 cm^{-1} (cellulosic compounds band) (*12*). McLeod had the lowest ($P < 0.05$) value in total CHO peak area (62.68), and CDC Helgason had the highest total carbohydrate peak area (76.71).

The three characteristic absorption peaks that fell in the CHO region (ca. 1184−951 cm^{-1}) (**Figure 2**) were analyzed, and similar trends was observed. McLeod had the smallest ($P < 0.01$) area of the first CHO peak (7.03), in contrast to CDC Dolly and CDC Helgason (8.67 and 9.02, respectively). Compared to the other varieties, McLeod and CDC Helgason exhibited relatively lower ($P < 0.05$) peak heights of the first CHO peak (0.24 and 0.27, respectively). There was no difference ($P > 0.05$) in the second

Article

J. Agric. Food Chem., Vol. 58, No. 13, 2010 **7805**

Table 2. Structural Characteristics of Protein Amides I and II and Carbohydrates, and Structural Carbohydrate (Cellulosic Compounds) in the Endosperm Tissue of Barley Varieties, Revealed Using Synchrotron-Based FTIR Microspectroscopy: Comparison of Six Barley Varieties

items	peak (cm⁻¹)	region (cm⁻¹)	baseline (cm⁻¹)	AC Metcalfe	CDC Dolly	McLeod	CDC Helgason	CDC Trey	CDC Cowboy	SEM[a]	P value
				characteristics of whole barley seed in terms of the mid-IR absorbed peak area, height, and their ratios (infrared absorbed intensity unit)							
				amide molecular spectral features							
				based on the amide I and II peak area, and height							
amide I peak area	~1650	1722–1578	1722–1487	7.99 bc	8.23 abc	10.02 a	7.33 c	9.01 ab	9.23 ab	0.582	0.004
amide I peak height	~1650	1722–1578	1722–1487	0.11 cd	0.12 bcd	0.16 a	0.11 d	0.14 ab	0.13 bc	0.091	<0.0001
amide II peak area	~1550	1578–1487	1722–1487	1.94 b	1.97 abc	2.57 a	1.86 b	2.20 ab	2.34 a	0.182	0.024
amide II peak height	~1550	1578–1487	1722–1487	0.04 b	0.04 ab	0.05 a	0.04 b	0.04 ab	0.04 ab	0.004	0.133
amide I and II area		1722–1487	1722–1487	9.93 bc	10.20 abc	12.59 a	9.19 c	11.22 ab	11.56 a	0.754	0.005
				carbohydrate (CHO) molecular spectral features							
				based on the carbohydrate peak area and height							
cellulosic compound area	~1240	1273–1217	1273–1217	0.54 a	0.53 ab	0.48 b	0.54 a	0.47 b	0.49 b	0.020	0.003
cellulosic compound height	~1240	1273–1217	1273–1217	0.02 ab	0.02 a	0.02 b	0.02 ab	0.02 b	0.02 b	0.002	0.121
total carbohydrate peak area		1184–951	1184–951	71.10 a	75.20 a	62.68 b	76.71 a	72.30 a	72.31 a	2.889	0.022
CHO: 1st component peak area	~1150	1184–1132	1184–951	8.25 b	8.67 ab	7.03 c	9.02 a	8.14 b	8.19 b	0.374	0.006
CHO: 1st component peak height	~1150	1184–1132	1184–951	0.29 a	0.30 ab	0.24 b	0.27 ab	0.28 a	0.28 a	0.012	0.048
CHO: 2nd component peak area	~1080	1132–1066	1184–951	10.41 ab	11.24 a	9.54 b	11.14 a	10.74 ab	10.64 ab	0.460	0.175
CHO: 2nd component peak height	~1080	1132–1066	1184–951	0.42 ab	0.45 a	0.38 b	0.44 a	0.42 ab	0.42 ab	0.017	0.144
CHO: 3rd component peak area	~1025	1066–951	1184–951	44.92 b	47.38 ab	39.59 c	48.66 a	46.08 ab	46.30 ab	1.791	0.014
CHO: 3rd component peak height	~1025	1066–951	1184–951	0.66 ab	0.69 ab	0.59 b	0.72 a	0.72 a	0.72 a	0.029	0.014

[a] SEM = pooled standard error of means. Means with different letters in the same row are significantly different (P < 0.05).

Table 3. Structural Characteristics of the Ratios of Amides I and II, and Structural (Cellulosic Compounds) and Nonstructural (NSC, Starch) Carbohydrates (CHO) in the Endosperm Tissue of Barley Varieties, Revealed Using Synchrotron-Based FTIR Microspectroscopy: Comparison of Six Barley Varieties

items	peaks area regions (baseline) (cm^{-1})	molecular characteristics of barley seed in terms of the mid-IR absorbed peak area and height and their ratios (IR absorbed intensity unit)						SEM^a	P value
		AC Metcalfe	CDC Dolly	McLeod	CDC Helgason	CDC Trey	CDC Cowboy		
		based on the amide I and CHO peak area and height ratios							
ratio of total CHO peak area/amides I and II peak area	1184−951 (baseline: 1184−951)/1722−1487 (baseline 1722−1487)	8.90 b	9.15 abc	7.11 c	9.89 ab	10.81 a	9.49 ab	0.618	0.002
ratio of NSC (starch) peak area (CHO 3rd peak)/amides I peak area	1066−951 (baseline:1184−951)/1722−1487 (baseline 1722−1487)	6.91 b	6.86 abc	5.35 c	7.68 ab	8.25 a	7.58 ab	0.505	0.003
ratio of NSC (starch) peak height (CHO 3rd peak)/amide I height	~1025 (baseline: 1184−951)/~1650 (baseline: 1722−1487)	6.91 bc	7.24 bc	5.16 c	7.90 b	8.41 ab	9.97 a	0.789	<0.001
ratio of amides I and II peak area/cellulosic compound peak area	1722−1487 (baseline: 1722−1487)/1273−1217 (baseline: 1273−1217)	19.41 b	20.98 ab	26.44 a	17.99 b	23.64 a	24.29 a	1.568	<0.0001
ratio of amide I peak area/cellulosic compound peak area	1722−1587 (baseline: 1722−1487)/1273−1217 (baseline: 1273−1217)	15.44 b	16.92 ab	21.03 a	14.27 b	18.96 a	19.36 a	1.190	<0.0001
ratio of amide I peak height/cellulosic compound peak height	~1650 (baseline: 1722−1487)/1273−1217 (baseline: 1273−1217)	5.90 c	6.36 bc	9.77 a	5.67 c	7.87 b	7.67 b	0.501	<0.0001
ratio of total CHO peak area/cellulosic compound peak area	1184−951 (baseline: 1184−951)/1273−1217 (baseline: 1273−1217)	137.14 bc	144.80 abc	130.89 c	144.99 abc	157.57 a	148.60 ab	5.963	0.022
ratio of NSC (starch) peak area (CHO 3rd peak) /cellulosic peak area	1066−951 (baseline: 1184−951)/1273−1217 (baseline: 1273−1217)	87.08 bc	91.26 abc	82.65 c	92.71 abc	101.24 a	95.32 ab	3.936	0.011
ratio of NSC (starch) peak height (CHO 3rd peak)/cellulosic peak height	~1025 (baseline: 1184−951)/1273−1217 (baseline: 1273−1217)	34.56 d	36.47 cd	35.82 cd	38.45 bc	42.47 a	40.93 ab	1.271	<0.0001

^{a} SEM = pooled standard error of means. Means with different letters in the same row are significantly different ($P < 0.05$).

Article

J. Agric. Food Chem., Vol. 58, No. 13, 2010 **7807**

CHO peak intensity shown here. At ca. 1066–951 cm^{-1}, there was an absorption band, which was assigned to nonstructural starch. The peak maxima appeared at ca. 1025 cm^{-1} (*12*). Consistent with other CHO peak parameters, McLeod had the smallest ($P < 0.05$) third CHO peak area and relatively smaller peak height (0.59), suggesting the lowest enrichment of starch in endosperm tissue among the six barley varieties. Starch is abundant in endosperm tissue with different granule size, type, and content (*28, 29*). These variable molecular characteristics of barley endosperm tissue may have a strong influence on ruminal fermentation and degradation.

Structural Characteristics of the Ratios of Amides I and II, and Structural and Nonstructural Carbohydrates (CHO) in Barley Endosperm. In order to further understand the structural and chemical makeup of the barley endosperm, relative peak intensity ratios of specific bands associated with nutrients were calculated and presented in **Table 3**. The ratio analysis was calculated using the infrared absorbance intensity (area or height) of one characteristic peak observed in the spectrum to divide that of another one. The results show that McLeod had the relatively smaller ratio of total CHO peak area to amides I and II peak area (7.11). The ratios of nonstructural carbohydrate starch (ca. 1205 cm^{-1}) to amide I (at 1650 cm^{-1}) were significantly different among the six barley varieties. McLeod showed a relatively smaller value for both the area and height ratio comparisons (5.35 and 5.16, respectively). According to the chemical composition analysis, McLeod has relatively more protein and less CHO content, which may be a reason for the smallest CHO/amide ratio. Varlier, feed-type barley variety, was found to have a lower starch/protein ratio in an earlier study, implying that protein protects starch from degradation in rumen (*30*).

There was also a notable difference in the ratio of the amide band to cellulosic compounds in the 1273–1217 cm^{-1} region. CDC Helgason, AC Metcalfe, and CDC Dolly had relatively smaller ratios of amide I/cellulosic peak area (14.27, 15.44, and 16.92, respectively). The same trend was also found in the peak area ratio comparison of amide I/cellulosic compounds. McLeod had the greatest ($P < 0.05$) height ratio of amide I/cellulosic compounds (9.77). This is further evidence to support the opinion that cellulosic compounds significantly contribute to the lower digestibility and degradability.

Another large difference ($P < 0.05$) was seen at the peak area ratio of total CHO/cellulosic compounds. The higher starch content and lower undigestible fibrous materials may result in the better nutrient value, which has been noted in an earlier study (*31*). In comparison with CDC Trey (157.57) and CDC Cowboy (148.60), McLeod was merely 130.89. The ratio of nonstructural CHO (starch) peak area (CHO third peak)/cellulosic compounds peak area exhibited a similar trend among these six barley varieties. CDC Trey and CDC Cowboy had a relatively higher ($P < 0.05$) peak height ratio of nonstructural CHO (starch) peak area (CHO third peak)/cellulosic compounds (42.47 and 40.93, respectively). Others ranged from 34.56 to 38.45.

Protein matrix provides adhesion for starch granules in endosperm tissue (*32*). Cellulosic compounds in the cell wall also make an effort to support and maintain microstructure. This association may influence the hardness of cereal, the particle size distribution, and, as a result, nutrition value. With protein encompassing the starch granules, cultivars containing more protein may be associated with harder structure. The protein content, structure, distribution, and conjunction may partially explain the grain characteristics. Whereas, documents are lacking in individual spot sampling on barley grain using IR spectroscopic analysis. Little information is comparable. Further study is

needed to examine whether this can be used to predict the nutrient availability of grain.

We can draw the conclusion that in conjunction with synchrotron light source, chemical–structural information can be obtained in situ via the synchrotron FTIRM technique with intact tissue sections. Compared to traditional chemical analysis methodologies, for which grinding is always required, synchrotron SFTIRM is obviously superior in probing the internal biological matrix with minimal artificial influence within a cellular dimension. Again, the results confirm that with the advanced synchrotron FTIRM techniques, chemical–structural information of feedstuffs can be revealed. The synchrotron FTIRM data can provide the structural–chemical makeup information of original biological tissue.

Correlations between in Situ Degradation Kinetics (Rate and Extent) and Spectral Characteristics among Barley Varieties. Pearson correlation was computed to investigate the relationship between the synchrotron FTIRM spectral data and the rumen degradation rate and extent of DM, CP, and ST (**Tables 4** and **5**), and the soluble fraction (S) and potentially degradable fraction (D) of DM, CP, and ST in **Table 6** for the evaluation of nutrient availability. The results showed that the correlation tendency appeared between the synchrotron FTIRM data and degradation features, though not all of them were significant (**Tables 4–6**). For CHO, the first component peak area was correlated with the degradation rate (K_d) of CP ($P = 0.101$) (**Table 4**). Cellulosic compound area was correlated with soluble fractions (S, %) of CP ($P = 0.068$) and ST ($P = 0.041$) (**Table 6**). Additional spectroscopic analysis is necessary to clarify this assumption as to whether the chemical–structural makeup of the endosperm tissue is linked to the degradation kinetics of cereals grain.

Weak correlations (**Tables 4–6**) indicate that limited variations of these six barley varieties might not be sufficient to interpret the relationship between spectroscopic information and nutrient value of barley grain, although significant differences in the biodegradation kinetics were observed as presented in **Table 1**. The weak correlations may be due to the similarities and fewer variations among the barley varieties and may also be due to the limited number barley varieties (only six barley varieties were examined). The differences among the samples may not be significant enough to reveal the actual relationship between the spectroscopic data and the ruminal degradation kinetics (rate and extent). More studies involving a diverse range of samples with biological differences will, thereby, be necessary to further understand the relationship between the mid-IR spectroscopic information and nutrition value of feedstuffs.

In conclusion, inherent structural differences in the endosperm tissue among the seeds of the six barley varieties were detected by the synchrotron-based FTIRM technique with the univariate molecular spectral analysis. The synchrotron FTIRM spectral profiles differed among the barley varieties. The studies demonstrated the potential of ultraspatially resolved synchrotron based analytical technology (SFTIRM) to reveal the structural and chemical makeup within cellular and subcellular dimensions without destruction of the inherent structure of cereal seed tissue. With the synchrotron FTIRM technique, the structural characteristics of the cereal seeds were illuminated among different cultivars at high spatial resolution. The structural differences of barley seeds may be one reason for the various digestive behaviors and nutritive values for ruminants. Examination of other tissues such as seed coat, aleurone layer, and pericarp in barley may provide further insight as to why barley varieties exhibit different biodegradation behaviors and provide a deeper and better indication of the chemical makeup and structural information. Weak correlations indicate that limited

7808 *J. Agric. Food Chem.,* Vol. 58, No. 13, 2010

Liu and Yu

Table 4. Pearson Correlation between Structural Characteristics from Seed Endosperm Tissue and in Situ Rumen Degradation Rate and Extent of Six Barley Varieties[a]

	in situ rumen degradation kinetics of DM[b]				in situ rumen degradation kinetics of CP[b]				in situ rumen degradation kinetics of ST[b]			
	K_d (%/h)		EDDM (%)		K_d (%/h)		EDCP (%)		K_d (%/h)		EDST (%)	
items	correlation coefficient	*P*-value	correlation coefficient	*P*-value	correlation coefficient	*P*-value	correlation coefficient	*P*-value	correlation coefficient	*P*-value	correlation coefficient	*P*-value
amide I peak area	0.610	0.198	0.529	0.281	0.644	0.168	0.538	0.271	0.381	0.456	0.394	0.440
amide I peak height	0.569	0.239	0.463	0.355	0.625	0.185	0.480	0.335	0.330	0.523	0.317	0.540
amide II peak area	0.498	0.315	0.434	0.390	0.513	0.298	0.437	0.386	0.290	0.578	0.312	0.547
amide II peak height	0.513	0.298	0.443	0.379	0.512	0.299	0.448	0.373	0.324	0.531	0.329	0.524
amide I and II area	0.587	0.220	0.510	0.302	0.617	0.192	0.517	0.293	0.362	0.480	0.377	0.461
cellulosic compound area	−0.511	0.300	−0.553	0.255	−0.560	0.247	−0.550	0.258	−0.321	0.535	−0.418	0.410
cellulosic compound height	−0.349	0.497	−0.0522	0.288	−0.257	0.623	−0.494	0.320	−0.347	0.500	−0.480	0.336
CHO: 1st component peak area	−0.711	0.113	−0.556	0.252	−0.728	0.101	−0.582	0.225	−0.515	0.296	−0.435	0.389
CHO: 1st component peak height	−0.021	0.968	0.058	0.914	−0.059	0.912	0.045	0.933	0.097	0.855	0.140	0.792
CHO: 2nd component peak area	−0.646	0.166	−0.505	0.307	−0.609	0.199	−0.528	0.282	−0.527	0.283	−0.426	0.399
CHO: 2nd component peak height	−0.630	0.180	−0.503	0.309	−0.610	0.199	−0.523	0.287	−0.484	0.331	−0.407	0.423
CHO: 3rd component peak area	−0.660	0.154	−0.449	0.372	−0.687	0.132	−0.486	0.329	−0.471	0.346	−0.336	0.515
CHO: 3rd component peak height	−0.509	0.302	−0.201	0.702	−0.579	0.229	−0.255	0.626	−0.313	0.546	−0.098	0.853
Total carbohydrate peak area	−0.668	0.147	−0.484	0.330	−0.680	0.137	−0.515	0.295	−0.487	0.327	−0.374	0.465

[a] The structural characteristics include protein amides I and II and carbohydrates and structural carbohydrate (cellulosic compounds) in the endosperm tissue of barley varieties, revealed using synchrotron-based FTIR microspectroscopy. [b] K_d = degradation rate; EDDM, EDCP, and EDST = effective degradability of DM, CP, and starch, respectively.

Table 5. Pearson Correlation Results between Structural Characteristic Ratios from Seed Endosperm Tissue and in Situ Rumen Degradation Rate and Extent of Six Barley Varieties[a]

	in situ rumen degradation kinetics of DM[b]				in situ rumen degradation kinetics of CP[b]				in situ rumen degradation kinetics of ST[b]			
	K_d (%/h)		EDDM (%)		K_d (%/h)		EDCP (%)		K_d (%/h)		EDST (%)	
items	correlation coefficient	*P*-value	correlation coefficient	*P*-value	correlation coefficient	*P*-value	correlation coefficient	*P*-value	correlation coefficient	*P*-value	correlation coefficient	*P*-value
ratio of total CHO peak area/amides macl and II peak area	−0.279	0.593	0.030	0.955	−0.322	0.533	−0.012	0.982	−0.098	0.853	0.102	0.848
ratio of NSC (starch) peak area (CHO 3rd peak)/amides I peak area	−0.295	0.571	0.045	0.933	−0.380	0.457	−0.007	0.990	−0.081	0.879	0.138	0.795
ratio of NSC (starch) peak height (CHO 3rd peak)/amide I height	−0.294	0.572	0.042	0.937	−0.434	0.390	−0.026	0.961	−0.109	0.837	0.143	0.788
ratio of amides I and II peak area/ cellulosic compound peak area	0.552	0.256	0.489	0.325	0.596	0.212	0.495	0.319	0.317	0.540	0.351	0.495
ratio of amide I peak area/cellulosic compound peak area	0.555	0.253	0.489	0.325	0.607	0.202	0.496	0.317	0.315	0.544	0.348	0.499
ratio of amide I peak height/cellulosic compound peak height	0.509	0.303	0.413	0.415	0.574	0.234	0.428	0.398	0.263	0.614	0.264	0.613
ratio of total CHO peak area/cellulosic compound peak area	−0.171	0.746	0.117	0.826	−0.175	0.741	0.076	0.887	−0.089	0.867	0.136	0.797
ratio of NSC (starch) peak area (CHO 3rd peak) /cellulosic peak area	−0.169	0.750	0.139	0.793	−0.190	0.718	0.094	0.860	−0.069	0.896	0.165	0.754
ratio of NSC (starch) peak height (CHO 3rd peak)/cellulosic peak height	−0.125	0.813	0.185	0.726	−0.155	0.770	0.134	0.801	−0.085	0.873	0.177	0.737

[a] The structural characteristics include protein amides I and II, and structural (cellulosic compounds) and nonstructural (NSC, starch) carbohydrates (CHO) in the endosperm tissue of barley varieties, revealed using synchrotron-based FTIR microspectroscopy. [b] K_d = degradation rate; EDDM, EDCP, and EDST = effective degradability of DM, CP, and starch, respectively.

variations of these six barley varieties might be not sufficient to interpret the relationship between synchrotron-based mid-IR spectroscopic information and the nutrient value of barley grain, although significant differences in the biodegradation kinetics were observed. Further research will be focused on the relationship between mid-IR spectral information in a whole IR region from 4000 to 800 cm^{-1} (*not* individual peaks and ratios) and rumen degradation kinetics at the different tissues, not only endosperm but also pericarp, seed coat, and aleurone.

Article

J. Agric. Food Chem., Vol. 58, No. 13, 2010 **7809**

Table 6. Pearson Correlation Results between Structural Characteristics from Seed Endosperm Tissue and in Situ Rumen Degradation Characteristics (Soluble and Potentially Degradable Fractions) of Six Barley Varieties[a]

items	degradation characteristics of DM[b]				degradation characteristics of CP[b]				degradation characteristics of ST[b]			
	S (%)		D (%)		S (%/)		D (%)		S (%/)		D (%)	
	correlation coefficient	*P*-value	correlation coefficient	*P*-value	correlation coefficient	*P*-value	correlation coefficient	*P*-value	correlation coefficient	*P*-value	correlation coefficient	*P*-value
cellulosic compound area	−0.614	0.195	−0.281	0.590	0.779	0.068	−0.507	0.304	0.830	0.041	−0.677	0.140
cellulosic compound height	−0.527	0.283	−0.628	0.182	0.500	0.313	−0.823	0.044	0.404	0.427	−0.684	0.134
ratio of amide I peak area/cellulosic compounds peak area	0.442	0.380	0.035	0.948	−0.648	0.164	0.213	0.685	−0.860	0.028	0.531	0.278

[a] The structural characteristics include structural carbohydrate (cellulosic compounds) and amide I: cellulosic compound ratio in the endosperm tissue of barley varieties, revealed using synchrotron-based FTIR microspectroscopy. [b] S = soluble fraction; D = potentially degradable fraction of DM, CP, and starch.

LITERATURE CITED

(1) Hart, K. J.; Rossnagel, B. G.; Yu, P. Chemical characteristics and in situ ruminal parameters of barley for cattle: Comparison of the malting cultivar AC Metcalfe and five feed cultivars. *Can. J. Anim. Sci.* **2008**, *88*, 711–719.

(2) Liu N. Ruminal Nutrient Availability and Inherent Structural Features of Six Barley Varieties Using in Situ Technique and Mid-IR Spectroscopy. M.S. Thesis, University of Saskatchewan, Saskatoon, Canada, 2009.

(3) Wetzel, D. L.; LeVine, S. M. *Infrared Microbeam Analysis of Intricate Biological Specimens.* Institute of Physics: Philadelphia, PA, 2000; pp 65−66.

(4) Wetzel, D. L.; LeVine, S. M. Biological Applications of Infrared Microscopy. In *Infrared and Raman Spectroscopy of Biological Materials*; Gremlich, H.-U. , Yan, B., Eds.; Marcel Dekker Inc.: New York, 2001; pp 101−142.

(5) Budevska, B. O. Vibrational Spectroscopy Imaging of Agricultural Products. In *Handbook of Vibrational Spectroscopy*; Chalmers, J. M., Griffiths, P. R., Eds.; J. Wiley: Hoboken, NJ, 2002; pp 3720−3732.

(6) Diem, M.; Romeo, M.; Matthäs, C.; Miljkovic, M.; Miller, L.; Lasch, P. Comparison of Fourier transform infrared (FTIR) spectra of individual cells acquired using synchrotron and conventional sources. *Infrared Phys. Technol.* **2004**, *45* (5−6), 331–338.

(7) Miller, L. M.; Carr, G. L.; Jackson, M.; Dumas, P.; Williams, G. P. The impact of infrared synchrotron radiation in biology: Past, present and future. *Synchrotron Radiation News* **2000**, *13*, 31–38.

(8) Marinkovic, N. S.; Huang, R.; Bromberg, P.; Sullivan, M.; Sperber, E.; Moshe, S.; Miller, L. M.; Jones, K.; Chouparova, E.; Franzen, S. Center for Synchrotron Biosciences' U2B Beamline: An international resource for biological infrared spectroscopy. *J. Synchrotron Radiat.* **2002**, *9* (part 4), 189–197.

(9) Yu, P. Application of advanced synchrotron radiation-based Fourier transform infrared (SR-FTIR) microspectroscopy to animal nutrition and feed science: a novel approach. *Br. J. Nutr.* **2004**, *92* (6), 869–885.

(10) Marinkovic, N. S.; Chance, M. R. Synchrotron Infrared Microspectroscopy. In *Encyclopedia of Molecular Cell Biology and Molecular Medicine*; Meyers, R., Ed.; Wiley: New York, 2005; pp 671−708.

(11) Miller, L. M.; Dumas, P. Chemical imaging of biological tissue with synchrotron infrared light. *Biochim. Biophys. Acta* **2006**, *1758* (7), 846–857.

(12) Wetzel, D. L.; Eilert, A. J.; Pietrzak, L. N.; Miller, S. S.; Sweat, J. A. Ultraspatially-resolved synchrotron infrared microspectroscopy of plant tissue *in situ*. *Cell. Mol. Biol.* (*Noisy-Le-Grand*) **1998**, *44* (1), 145–168.

(13) Miller, L. M. Infrared Microspectroscopy and Imaging; National Synchrotron Light Source, Brookhaven National Laboratory, Internal Publication, 2002. http://www.nsls.bnl.gov/newsroom/publications/otherpubs/imaging/workshopmiller.pdf [accessed July, 2009].

(14) Yu, P.; Block, H.; Niu, Z.; Doiron, K. Rapid characterization of molecular chemistry, nutrient make-up and microlocation of internal seed tissue. *J. Synchrotron Radiat.* **2007**, *14* (part 4), 382–390.

(15) Dumas, P.; Miller, L. The use of synchrotron infrared microspectroscopy in biological and biomedical investigations. *Vib. Spectrosc.* **2003**, *32* (1), 3–21.

(16) Rossnagel, B. G.; Harvey, B. L. CDC Dolly two-row feed barley. *Barley Newsletter*; American Malting Barley Association, Inc.: Milwaukee, WI, 1994; Vol. 38, p109.

(17) Legge, W. G. AC Metcalfe barley. *Can. J. Plant Sci.* **2003**, *83* (2), 381–384.

(18) Yu, P.; Doiron, K.; Liu, D. Shining light on the differences in molecular structural chemical make-up and the cause of distinct degradation behavior between malting- and feed-type barley using synchrotron FTIR microspectroscopy: a novel approach. *J. Agric. Food Chem.* **2008**, *56* (9), 3417–3426.

(19) Walker, A, M.; Yu, P.; Christensen, C. R.; Christensen, D. A.; McKinnon, J. J. Fourier transform infrared microspectroscopic analysis of the effects of cereal type and variety within a type of grain on molecular structural make-up in relation to rumen degradation kinetics. *J. Agric. Food Chem.* **2009**, *57*, 6871–6878.

(20) Yu, P.; Christensen, D. A.; Christensen, C. R.; Drew, M. D.; Rossnagel, B. G.; McKinnon, J. J. Use of synchrotron FTIR microspectroscopy to identify chemical differences in barley endosperm tissue in relation to rumen degradation characteristics. *Can. J. Anim. Sci.* **2004**, *84* (3), 523–528.

(21) Doiron, K. J.; Yu, P.; Christensen, C. R.; Christensen, D. A.; McKinnon, J. J. Detecting molecular changes in vimy flaxseed protein structure using synchrotron ftirm and drift spectroscopic techniques: structural and biochemical characterization. *Spectroscopy* **2009**, *23*, 307–322.

(22) Doiron, K. J.; Yu, P.; McKinnon, J. J.; Christensen, D. A. Heat-induced protein structures and protein subfractions in relation to protein degradation kinetics and intestinal availability in dairy cattle. *J. Dairy Sci.* **2009**, *92*, 3319–3330.

(23) Pietrzak, L. N.; Miller, S. S. Microchemical structure of soybean seeds revealed *in situ* by ultraspatially resolved synchrotron Fourier transformed infrared microspectroscopy. *J. Agric. Food Chem.* **2005**, *53* (24), 9304–9311.

(24) Stuart, B. *Infrared Spectroscopy: Fundamentals and Applications*; J. Wiley: Chichester, England, 2004.

(25) Yu, P. Applications of hierarchical cluster analysis (CLA) and principal component analysis (PCA) in feed structure and feed

molecular chemistry research, using synchrotron-based Fourier transform infrared (FTIR) microspectroscopy. *J. Agric. Food Chem.* **2005**, *53* (18), 7115–7127.

(26) Camm, G. A. Grain Hardness and Slow Dry Matter Disappearance Rate in Barley. M.S. Thesis, University of Saskatchewan, Saskatoon, SK, Canada, 2008.

(27) Mikel, M. A.; Kolb, F. L. Genetic Diversity of Contemporary North American Barley. *Crop Sci.* **2008**, *48* (4), 1399–1407.

(28) Takeda, Y.; Takeda, C.; Mizukami, H.; Hanashiro, I. Structures of large, medium and small starch granules of barley grain. *Carbohydr. Polym.* **1999**, *38* (2), 109–114.

(29) You, S. G.; Izydorczyk, M. S. Molecular characteristics of barley starches with variable amylose content. *Carbohydr. Polym.* **2002**, *49* (1), 33–42.

(30) Yu, P. An emerging method for rapid characterization of feed structures and feed component matrix at a cellular level and relation to feed quality and nutritive value. *Arch. Anim. Nutr.* **2006**, *60* (3), 229–244.

(31) Bowman, J. G. P.; Blake, T. K.; Surber, L. M. M.; Habernicht, D. K.; Bockelman, H. Feed-quality variation in the barley core collection of the USDA National Small Grains Collection. *Crop Sci.* **2001**, *41* (3), 863–870.

(32) Holopainen, U. R.; Wilhelmson, A.; Salmenkallio-Marttila, M.; Peltonen-Sainio, P.; Rajala, A.; Reinikainen, P.; Kotaviita, E.; Simolin, H.; Home, S. Endosperm structure affects the malting quality of barley (*Hordeum vulgare* L.). *J. Agric. Food Chem.* **2005**, *53* (18), 7279–7287.